

Collision induced coherence in plasma and Branching Ratio in multilevel system

Dong Sun^{1,2,3}, Victor V. Kozlov^{3,4,+}, Lan Yuan¹, Yuri V. Rostovtsev^{3,5}

¹ Department of Optoelectronics Engineering,

Xiamen University of Technology, Xiamen 361024, China

² Fujian Provincial Key Laboratory of Optoelectronic technologies and devices,
Xiamen 361024, China

³ Department of Physics, Texas A&M University,
College Station, TX 77843

⁴ Fock Institute of Physics, St. -Petersburg University,
Ulyanovskaya 1, St.-Petersburg, Russia, 198904

⁵ Department of Physics, University of North Texas,
1155 Union Circle #311427, Denton, TX 76203
+ Deceased

(Dated: December 5, 2018)

Our work is based on the collision-induced coherence of two decay channels along two optical transitions. The quantum interference of pumping processes creates the dark state and the more atoms are pumped in this collision-induced dark state the stronger the suppression of the spontaneous emission. The efficiency of this suppression is quantified by putting it in comparison with the spontaneous emission on the ultraviolet transition which proceeds in a regular fashion. The branching ratio of these two (visible and ultraviolet) transitions is introduced as the effective measure of the degree of the suppression of the spontaneous emission on the visible transition. Our preliminary calculations show that a significant decrease of the branching ratio with increase of electron densities is reproduced in the theory.

PACS numbers: 42.50.Gy, 42.65.-k, 32.80.Qk

I. INTRODUCTION

An excited free atom decays into a vacuum emitting spatially isotropic radiation in the spectrum of frequencies which has Lorentzian shape with a bandwidth proportional to the Einstein A coefficient [1]. The decay rate is a combination of fundamental atomic constants and strongly resistant to a modification. However, such modifications are possible for instance of the strongly confined atom [2]. The rate is enhanced or suppressed through the modification of the density of electromagnetic modes in the neighborhood of the resonant frequency [3]-[5]. Using a three-level atom driven by coherent fields is another way to control the spontaneous emission [6] and observe narrowing of spectral linewidth compared to the natural linewidth [7, 8]. Four-level driven atomic configurations offer yet another level of control allowing, for example, spectral line elimination and full spontaneous emission cancellation [9, 10].

The topic of above-mentioned studies has been focused on individual transitions in atoms and addressed the modification of one or another rate of spontaneous radiative decay. A number of studies consider more involved schemes characterized by correlated emission simultaneously from two atomic upper levels. Such type of interference of decay channels has been exploited, for instance, by Harris in his proposal of lasing without inversion in [11]. In contrast to most studies, we consider not the direct interference of decay channels, but rather the interference of incoherent pumping rates (namely, collision-induced interference). In its turn, this interference induces the correlation in spontaneous emission. We propose using branching ratio R as the measure of this correlation. The term branching ratio here stands for the ratio of two spontaneous decay rates from two upper levels $|a\rangle$ and $|b\rangle$ to

two lower levels $|c\rangle$ and $|d\rangle$ in a five-level atom of Fig.1:

$$R = \frac{\gamma_{vis}}{\gamma_{UV}} \quad (1)$$

where for definition we formulate the branching ratio in terms of decay rates on visible, γ_{vis} , and ultraviolet, γ_{UV} , transitions. Here, we refer to particular transitions in order to keep a close link to the previous experiments on measurements of changes of branching ratios. These experiments were performed in plasmas in Princeton by Suckewer and coworkers [12]. They serve as the main motivation and reference point of our study, although our results are applicable to more general schemes.

The branching ratio is closely related to total spectral-line intensities (in photons) for the two transitions, I_{vis} and I_{UV} . This relation is simply the consequence of the fact that the intensities are proportional to corresponding decay rates (for schemes considered so far): $I_{vis} \propto \gamma_{vis}$ and $I_{UV} \propto \gamma_{UV}$. In fact, this proportionality allows us to consider the intensity as alternative operational definition of the decay rate which differs from the pure decay rate by a factor. The access to this factor can be, however, a difficult experimental task. This potential experimental problem disappears when we consider the branching ratio. In those cases where the radiation is emitted from same level(s) the factors are the same for both transitions and therefore cancels out in the ratio in Eq. (1). So, the operational definition of the branching ratio can be introduced as

$$R = \frac{I_{vis}}{I_{UV}} \quad (2)$$

Moreover, for some cases, including ours, the operational definition in Eq. (2) is very natural and probably the only

possible definition. The problem is that we consider simultaneous decay along two (visible) transitions. This decay is characterized by more than one decay rate. This problem does not appear for the ultraviolet radiation, the decay of which happens along one transition and is therefore characterized by a single decay rate. However, we cannot formulate the branching ratio in the form of Eq. (1); and instead, we characterize the spontaneous emission process by the operational definition given by Eq. (2).

For optically thin samples and decays from common upper level, the equality between two definitions Eqs. (1) and (2), i.e. the equality between the ratio of line intensities and the ratio of the corresponding decay rates, points to the way of measurements of decay rates. Thus, from measurements of the intensity ratio of two lines, the ratio R and one of the spontaneous decay rates can be deduced knowing the other. Such spectroscopic technique is rather popular in plasma physics. Particularly attractive is the fact that the branching ratio is as immune to environmental conditions as the decay rate is. For instance, the ratio does not depend on the electron density and temperature. In the experiments of [12], it is reported that for some transitions the branching ratio becomes the function of density (concentration). They interpreted this observation as quenching of spontaneous-emission coefficients for visible transitions. Our study is devoted to formulation of the problem in quantum-optical terms, and our model is based on the five-level scheme (see Fig. 1), and the effect is caused by collision-induced quantum coherence between two upper levels.

The best way to formulate our main result is to compare two cases. The first one corresponds to no coherence between upper levels a and b . Then, the branching ratio for visible and ultraviolet transition found from the operational definition (2) reads

$$R = 2 \frac{\gamma_{vis}}{\gamma_{UV}} \quad (3)$$

as found in the following sections. Here the difference in the factor of two from original definition (1) arises due to doubling the visible decay rate (here $\gamma_a = \gamma_b \equiv \gamma_{vis}$) by taking into account decays from both upper levels (with equal rates). In contrast, the rate on the ultraviolet transition is not doubled because the spontaneous decay originates from single level a . Apart from this factor, the equation (3) stands in line with regular expectations. In particular, this result is unable to explain the concentration dependence of R reported in [12].

The second case realizes when the (maximal) coherence between levels a and b is induced by electron collisions. Then, as we shall show in the following sections, the branching ratio under steady-state conditions is given by

$$R = \gamma_{vis} \left(\frac{4}{r_e} + \frac{1}{r_{vis}} \right) = \frac{\gamma_{vis}}{N} \sqrt{\frac{\pi M}{kT}} \left(\frac{2e^{\frac{E_e}{kT}}}{\bar{k}_e} + \frac{e^{\frac{E_a}{kT}}}{2\bar{k}_{vis}} \right) \quad (4)$$

where, for simplicity, the result is evaluated in the limit of large pumping rates: $r_{vis}, r_e \gg \gamma_{vis}, \gamma_{UV}$; and k_i is the appropriate cross-sections of electronic excitation. Since all involved pumping rates depend on the electron concentration,

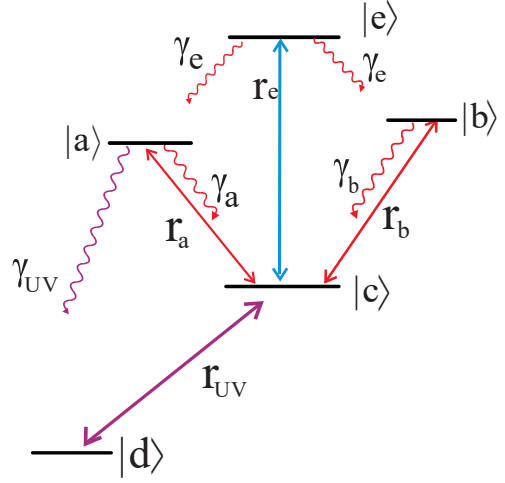


FIG. 1: Five-level configuration of working levels. Here γ_a and γ_b are spontaneous decay rates and r_a and r_b are collision-assisted pumping rates. The $|a\rangle \leftrightarrow |d\rangle$ is the ultraviolet transition with the spontaneous emission rate γ_{UV} . r_e is the pumping rate to state $|e\rangle$, γ_e is simultaneous equal decay rates to states $|a\rangle$ and $|b\rangle$. The rate r_d serves to close the system.

the branching ratio also becomes concentration-dependent. The higher the concentration the faster the pumping rates and therefore the lower the branching ratio. This relation implies quenching of spontaneous emission on the visible transition.

In the following sections we show that the effect of quenching is explained by creation of the collision-induced (i.e. induced by pumping rate r_{vis}) dark state as a linear combination of upper states a and b . By formulating the branching ratio R , all common dependencies cancel out and only the purified asymmetry of responses on the visible and ultraviolet transitions is left. Here, the branching ratio shows up as a valuable measure of the coherence-induced quenching of spontaneous emission on the visible transition.

II. BASIC SET OF EQUATIONS

We study the set of equations of motion governing temporal evolution of the density matrix elements for the five-level scheme shown in Fig. 1. The key ingredient of this scheme is the three-level V-type system consisting of two upper states $|a\rangle$, $|b\rangle$ connected to the lower state $|c\rangle$ by dipole allowed transitions. We first consider this three-level subsystem and then add two states $|d\rangle$ and $|e\rangle$. We assume that two transitions $|a\rangle - |c\rangle$ and $|b\rangle - |c\rangle$ have close transition frequencies and therefore upper states decay to same continuum of vacuum modes with decay constants γ_a and γ_b . These constants as well as details of the decay process follow from the Hamiltonian

$$V_\gamma = \hbar \sum_k g_k^{(a)} e^{i(\omega_{ac} - \nu_k)t} |a\rangle \langle c| \hat{a}_k + \hbar \sum_k g_k^{(b)} e^{i(\omega_{bc} - \nu_k)t} |b\rangle \langle c| \hat{a}_k + H.c. \quad (5)$$

describing interaction between the atom and the reservoir of vacuum oscillators, each of frequency ν_k (k here represents both the momentum and polarization of the vacuum mode). Here $g_k^{(a,b)}$ are the coupling constants between the k -th vacuum mode and the atomic transitions from $|a\rangle$ and $|b\rangle$ to $|c\rangle$. $\hat{a}_k(\hat{a}_k^\dagger)$ is the annihilation (creation) operator of a photon in the k -th vacuum mode, which obeys conventional bosonic commutation rule $[\hat{a}_k, \hat{a}_k^\dagger] = \delta_{kk'}$.

Electron collisions transfer atoms (also ions as in the plasma experiments in Ref. [12]) between states in the manner very much like that in the process of interaction with an optical field. As a consequence, the Hamiltonian appears in a similar form, as

$$V_R = \wp_{ac}\Omega|a\rangle\langle c| + \wp_{bc}\Omega|b\rangle\langle c| + H.c. \quad (6)$$

In contrast to coherent optical fields, individual collisional events are not correlated with each other and therefore the effective field Ω is incoherent. Note that spectrum of this incoherent field is very broad so that it covers both upper levels simultaneously, and therefore one and the same field drives both transitions. These transitions are characterized by dipole matrix elements \wp_{ac} and \wp_{bc} and transition frequencies ω_{ac} and ω_{bc} . The incoherent field has δ -like correlations at different times, i.e.,

$$\langle \Omega^*(t)\Omega(t') \rangle \propto \delta(t-t') \quad (7)$$

These correlations are not expected to cover the entire range of frequencies from $-\infty$ to $+\infty$. It is sufficient that they are at least approximately valid in the vicinity of both resonances and cover the frequency separation of two upper levels.

The total interaction picture Hamiltonian for the three-level subsystem is the sum of two terms introduced above,

$$H = V_\gamma + V_R \quad (8)$$

Derivation of equations of motion for the density matrix elements from the total Hamiltonian is a straightforward task. It is based on the scheme well developed in quantum optics, see for instance [13], where main ingredients are the Wigner-Weisskopf approximation and the generalized reservoir theory [14]. More details, particularly on the system under consideration, can be found in our paper [15]. With this reference to prior works we skip the derivation and jump

directly to the equations of motion. They read

$$\dot{\rho}_{aa} = -(r_a + \gamma_a)\rho_{aa} + r_a\rho_{cc} - \frac{1}{2}p\sqrt{r_ar_b}(\rho_{ba} + \rho_{ab}) \quad (9)$$

$$\dot{\rho}_{bb} = -(r_b + \gamma_b)\rho_{bb} + r_b\rho_{cc} - \frac{1}{2}p\sqrt{r_ar_b}(\rho_{ba} + \rho_{ab}) \quad (10)$$

$$\dot{\rho}_{cc} = (r_a + \gamma_a)\rho_{aa} + (r_b + \gamma_b)\rho_{bb} - (r_a + r_b)\rho_{cc} \quad (11)$$

$$+ p\sqrt{r_ar_b}(\rho_{ba} + \rho_{ab}) \quad (12)$$

$$\dot{\rho}_{ab} = -\frac{1}{2}(r_a + r_b + \gamma_a + \gamma_b)\rho_{ab} - i\Delta\rho_{ab} \quad (13)$$

$$+ \frac{1}{2}p\sqrt{r_ar_b}(2\rho_{cc} - \rho_{aa} - \rho_{bb}) \quad (14)$$

$$\dot{\rho}_{ca} = -\frac{1}{2}(2r_a + r_b + \gamma_a)\rho_{ca} - \frac{1}{2}p\sqrt{r_ar_b}\rho_{cb} \quad (15)$$

$$\dot{\rho}_{cb} = -\frac{1}{2}(2r_b + r_a + \gamma_b)\rho_{cb} - \frac{1}{2}p\sqrt{r_ar_b}\rho_{ca} \quad (16)$$

Here $r_{a,b} \equiv 2(\wp_{ac,bc}^2/\hbar^2)R$ are pumping rates of atoms to upper states $|a\rangle$ and $|b\rangle$ induced by collisions with electrons, see Fig. 1. Detuning $\Delta = \omega_{ac} - \omega_{bc}$ is supposed to be small as compared to the optical frequency and should be of the order of pumping rates r_a or r_b or less in order to make quantum interference effects observable.

Terms containing products of pumping rates appear due to the interference of two optical transitions which is induced by collisions with electrons. These terms are central to our discussion. In order to emphasize the role of this collision-induced interference, we assume that decay channels do not interfere. The interference terms are accompanied by the p factor. This factor is the normalized scalar product of corresponding dipole matrix elements:

$$p = \frac{\wp_{ac} \cdot \wp_{bc}}{|\wp_{ac}\wp_{bc}|} \quad (17)$$

According to its definition, the alignment factor takes the value equal to 1 for parallel dipole moments, -1 for antiparallel, and 0 for orthogonal. Intermediate values on $[-1, 1]$ segment are also possible. Maximal coherence corresponds to parallel or antiparallel dipole moments, while zero coherence corresponds to orthogonal dipole moments. These two extremes of maximal and minimal coherence deserve special attention.

It is not difficult to proceed with modeling the system shown in Fig. 1 and supplement the three-level subsystem with two additional levels. For further considerations we shall need only equations for populations and one equation for the polarization on $|a\rangle - |d\rangle$ transition. The upper state $|e\rangle$ is subject to decay with rate γ_e and pumping from state $|c\rangle$ by electronic collisions with rate r_e . So, for the population we immediately obtain

$$\dot{\rho}_{ee} = r_e(\rho_{cc} - \rho_{ee}) - 2\gamma_e\rho_{ee} \quad (18)$$

Of course, we could derive this equation from first principles by writing the Hamiltonian of interaction of the atom with the continuum of quantum oscillators to model the decay and interaction with the incoherent electron field to model the pumping process. Since no interference effects are expected on this transition, this derivation is no more than

a trivial exercise. The intuitive appearance of this equation stays in contrast to the detailed consideration of the V -type subsystem where the nontrivial appearance of interference terms requires cautious analysis.

Similar equation can be written for the lowest state of the system, $|d\rangle$. Here the decay with rate γ_{UV} from $|a\rangle$ state pumps the $|d\rangle$ state. The electron pumping is modeled by rate r_{UV} . So, in accordance with the picture in Fig. 1 we write

$$\dot{\rho}_{dd} = r_{UV}(\rho_{cc} - \rho_{dd}) + \gamma_{UV}\rho_{aa} \quad (19)$$

We now complete the set of equations by writing the equation of motion for the polarization on $|a\rangle - |d\rangle$ transition:

$$\dot{\rho}_{ad} = -\frac{1}{2}(\gamma_{UV} + r_{UV})\rho_{ad} \quad (20)$$

We can also write down equations of motion for the other polarizations involving states $|e\rangle - |d\rangle$. However, we do not do this because these equations are not used in further analysis. For more general considerations, if necessary, they can be composed by following directly the picture in Fig.1. Note that no interference terms appear.

To complete the model we should account for decays and pumpings between the V-subsystem and $|d\rangle$ and $|e\rangle$ states. The subset of equations (9)-(16) are modified in the following way. There is one incoming term for the population of $|b\rangle$ state: $+\gamma_e\rho_{ee}$. One incoming and one outgoing term for ρ_{aa} : $+\gamma_e\rho_{ee}$ and $-\gamma_{UV}\rho_{aa}$. For ρ_{cc} we get two additional pumping terms, $+r_e(\rho_{ee} - \rho_{cc})$ and $+r_{UV}(\rho_{dd} - \rho_{cc})$. The equation of motion for the two-photon coherence ρ_{ab} should be supplemented with decay term $\frac{1}{2}\gamma_{UV}\rho_{ab}$. One-photon polarization ρ_{ac} also decays faster due to additional decay term $\frac{1}{2}(r_e + r_{UV} + \gamma_{UV})\rho_{ac}$. Finally, in the equation for ρ_{bc} we should also write additional decay term $\frac{1}{2}(r_e + r_{UV})\rho_{bc}$. In the next section we summarize all these changes and after implementing a few simplified assumptions write down modified equations.

III. DRESSED-STATE ANALYSIS

We consider properties of the V-type subsystem $|a\rangle - |b\rangle - |c\rangle$ in the dressed-state picture. We assume equal dipole moments on $|a\rangle - |c\rangle$ and $|b\rangle - |c\rangle$ transitions for simplifications: $\wp_{ac} = \wp_{bc}$. This assumption immediately yields the equality of decay constants: $\gamma_a = \gamma_b$. We also get equal pumping rates, $r_a = r_b$. Also, let the two transitions have equal frequencies, so that two-photon detuning Δ is zero.

The upper level $|e\rangle$ is auxiliary with respect to the rest of the system. It serves to model the external pumping of two upper levels of the V -subsystem. In plasmas this pumping is due to thermal redistribution of population from all levels which are higher with respect to $|a\rangle$ and $|b\rangle$. In order to accurately account for details of this process we would have to consider a particular level scheme for a given atom/ion. However, our immediate goal is not the one-to-one description of a particular experiment but rather the proof-of-principle theoretical study of relevant coherent effects. Guided by simplicity we eliminate level $|e\rangle$ from our

five-level scheme. For that purpose, we assume fast decay rate γ_e with respect to pumping rate r_e . Then, from the equation (18) we can write for the population ρ_{ee} in steady-state:

$$\rho_{ee} \approx \frac{r_e}{\gamma_e}\rho_{cc} \quad (21)$$

With these simplifications in effect and additional terms from the discussion in the end of the previous section, equations (9)-(16) for the V -subsystem become

$$\dot{\rho}_{aa} = -(r_{vis} + \gamma_{vis} + \gamma_{UV})\rho_{aa} + (r_{vis} + \frac{r_e}{2})\rho_{cc} - pr_{vis}\rho_{ab} \quad (22)$$

$$\dot{\rho}_{bb} = -(r_{vis} + \gamma_{vis})\rho_{bb} + (r_{vis} + \frac{r_e}{2})\rho_{cc} - pr_{vis}\rho_{ab} \quad (23)$$

$$\dot{\rho}_{cc} = (r_{vis} + \gamma_{vis})(\rho_{aa} + \rho_{bb}) - (2r_{vis} + r_e + r_{UV})\rho_{cc} + 2pr_{vis}\rho_{ab} + r_{UV}\rho_{dd} \quad (24)$$

$$\dot{\rho}_{ab} = -(r_{vis} + \gamma_{vis} + \frac{\gamma_{UV}}{2})\rho_{ab} + \frac{1}{2}pr_{vis}(2\rho_{cc} - \rho_{aa} - \rho_{bb}) \quad (25)$$

with new notations: $\gamma_a = \gamma_b \equiv \gamma_{vis}$ and $r_a = r_b \equiv r_{vis}$. Here we write down only equations relevant for the study in this section. Equations for one-photon polarizations ρ_{ca} and ρ_{cb} will be considered in the next section.

Coherent effects in the V-subsystem appear due to the interference of pumping channels along $|a\rangle - |c\rangle$ and $|b\rangle - |c\rangle$ transitions. Actually, it is the same (incoherent) pumping process that drives both transitions. Here, the pumping field dresses atomic states $|a\rangle$ and $|b\rangle$ yielding the collision-induced dark state and its orthogonal partner-bright state with equal dipole moments $r_a = r_b$.

$$|D\rangle = \frac{1}{\sqrt{2}}(|a\rangle - |b\rangle) \quad (26)$$

$$|B\rangle = \frac{1}{\sqrt{2}}(|a\rangle + |b\rangle) \quad (27)$$

The equations of motion in terms of the dressed variables requires introduction of corresponding density matrix elements. They are

$$\rho_{DD} = \frac{1}{2}(\rho_{aa} + \rho_{bb} - 2\rho_{ab}) \quad (28)$$

$$\rho_{BB} = \frac{1}{2}(\rho_{aa} + \rho_{bb} + 2\rho_{ab}) \quad (29)$$

$$\rho_{DB} = \frac{1}{2}(\rho_{aa} - \rho_{bb}) \quad (30)$$

Given equations of motion in bare-states basis (22)-(25), and dressed-states definitions (28)-(30) for the density matrix elements, we reformulate these equations as

$$\dot{\rho}_{DD} = -\gamma_{vis}\rho_{DD} - \frac{\gamma_{UV}}{2}(\rho_{DD} + \rho_{DB}) + r_e\rho_{cc} \quad (31)$$

$$\dot{\rho}_{BB} = -(2r_{vis} + \gamma_{vis})\rho_{BB} - \frac{\gamma_{UV}}{2}(\rho_{BB} + \rho_{DB}) + (2r_{vis} + r_e)\rho_{cc} \quad (32)$$

$$\dot{\rho}_{DB} = -(r_{vis} + \gamma_{vis} + \frac{\gamma_{UV}}{2})\rho_{DB} - \frac{1}{4}\gamma_{UV}(\rho_{DD} + \rho_{BB}) \quad (33)$$

Our ultimate goal is the comparison of intensities of spontaneous emissions on the visible transition and on the ultraviolet transition. As we shall derive in the next section, these intensities are linearly proportional to the population of $|B\rangle$ state and $|a\rangle$ state, correspondingly. Both these populations can be obtained from the solution of equations (31)-(33) and inverted conversion formulas (28)-(30). It is not difficult to obtain exact steady-state solutions for all three dressed-states density matrix elements in above equations. However, we prefer to make yet another simplification in order to bring physics in the clearest possible form.

We assume that pumping rates are much faster than decay processes, particularly faster than the fastest decay rate γ_{UV} . Note that the spontaneous emission rate γ_{UV} is two orders of magnitude greater than decay rate γ_{vis} on the visible transition. Clearly, this difference is attributed to the cubic dependence of spontaneous decay rates on the transition frequency. In its turn, the high efficiency of pumping processes arises from frequent collisions of ions with free electrons (note that the electron concentration N_e exceeds the value of 10^{18} cm^{-3}). Finally, we formulate our assumption in the form of strong inequality

$$r_{vis}, r_e \gg \gamma_{UV}, \gamma_{vis} \quad (34)$$

This inequality is the key to understanding the effect of suppression of spontaneous emission on the visible transition. This understanding comes from the analysis of the equation (31). We shall see that more atoms in the dark state makes the emission weaker. The first two terms in equation (31) stand for the depletion of the dark state and are therefore undesirable for our purposes. [Note that steady-state polarization ρ_{DB} contributes as little as $(\gamma_{UV}/r_{vis})\rho_{DD}$.] This depletion is counterbalanced by the gain associated with the last term. The large value of this term requires fast pumping rate that is guaranteed by inequality (34).

With inequality (34) we get approximate solutions of equations (31)-(33). They are

$$\rho_{DD} \approx \frac{r_e}{\gamma_{UV}} \rho_{cc} \quad (35)$$

$$\rho_{BB} \approx (1 + \frac{r_e}{4r_{vis}}) \rho_{cc} \quad (36)$$

$$\rho_{DB} \approx \frac{r_e}{r_{vis}} \rho_{cc} \quad (37)$$

where we also used $\gamma_{UV} \gg \gamma_{vis}$. All these solutions are expressed in terms of ρ_{cc} which remains unknown quantity until we solve all equations of motion for the closed five-level system. However, the explicit knowledge of ρ_{cc} is not necessary for our study.

Solution (35) shows that the dark state is populated only due to the pumping via auxiliary upper state $|e\rangle$. By comparing solutions given by formulas (35) and (36) and using inequality (34), we conclude that $\rho_{DD} \gg \rho_{BB}$, so that the population of upper states $|a\rangle$ and $|b\rangle$ is dominantly concentrated in the dark state. This asymmetry means that most atoms are trapped in the non-emitting state $|D\rangle$. As we shall

see shortly, the spontaneous emission on the visible transition is proportional to ρ_{BB} ; and therefore basing on the just derived strong inequality $\rho_{DD} \gg \rho_{BB}$, we conclude that the emission is strongly suppressed. This suppression is to be put in comparison with the regular (unsuppressed) emission on the ultraviolet transition, which is regulated by the amount of population in the $|a\rangle$ state. Overall, the degree of suppression is quantitatively estimated by the corresponding branching ratio, as the ratio of two emissions, see Eq. (2) and derivations in the next section.

The population of the $|a\rangle$ state as well as ρ_{bb} and ρ_{ab} can be found by inverting definitions (28)-(30). So, in terms of bare states we get

$$\rho_{aa} = \frac{1}{2}(\rho_{BB} + \rho_{DD} + 2\rho_{DB}) \approx \frac{r_e}{2\gamma_{UV}} \rho_{cc} \quad (38)$$

$$\rho_{bb} = \frac{1}{2}(\rho_{BB} + \rho_{DD} - 2\rho_{DB}) \approx \frac{r_e}{2\gamma_{UV}} \rho_{cc} \quad (39)$$

$$\rho_{ab} = \frac{1}{2}(\rho_{BB} - \rho_{DD}) \approx -\frac{r_e}{2\gamma_{UV}} \rho_{cc} \quad (40)$$

This state is the state of maximal coherence in the sense that $|\rho_{ab}| \approx \sqrt{\rho_{aa}\rho_{bb}}$. This coherence is of collisional nature and its high degree is the reflection of the high efficiency of the pumping mechanism (r_{vis}).

IV. SPONTANEOUS EMISSION SPECTRA

We calculate the spectrum $S_{vis}(\omega)$ of spontaneously emitted photons on the visible transition, i.e. through $|a\rangle - |c\rangle$ and $|b\rangle - |c\rangle$ channels. Then, we similarly calculate the ultraviolet spectrum $S_{UV}(\omega)$ of photons emitted in the $|a\rangle - |d\rangle$ channel. Integrating these two spectra over the frequencies in the vicinity of the corresponding emission peaks and normalizing to the energy of one photon, we thus obtain two spectral-line intensities

$$I_{vis} = (\hbar\omega_{vis})^{-1} \int d\omega S_{vis}(\omega) \quad (41)$$

$$I_{UV} = (\hbar\omega_{UV})^{-1} \int d\omega S_{vis}(\omega) \quad (42)$$

In the case of three levels the calculation procedure quickly becomes cumbersome and requires numerical analysis on the final stage[16]. In our case the system is driven by an incoherent field that makes the situation a little simpler. Furthermore, applying the so far discussed approximations and simplifications, we can make the problem even analytically tractable with transparent final result. We even bypass the direct application of the quantum regression theorem.

First, we take the definition of the spectrum (valid for stationary processes) as the Fourier transform of the autocorrelation function of the second order of the scattered electric field:

$$S(\omega) = \frac{1}{\pi} \text{Re} \int_0^\infty d\tau e^{-i\omega\tau} \langle E^-(r, t) \cdot E^+(r, t + \tau) \rangle \quad (43)$$

This autocorrelation function is simply related to the normally-ordered product of polarizations taken at instants of time separated by a positive time delay τ . This relationship follows from the well-known formula

$$E^+(r, t) = -\frac{\omega_0^2}{4\pi\epsilon_0 c^2 r} \mathbf{n} \times (\mathbf{n} \times \mathbf{d}) \mathbf{P}^{(+)}(t - r/c) \quad (44)$$

connecting the electric field $\mathbf{E}^{(+)}$ with polarization $\mathbf{P}^{(+)}$. Here, \mathbf{n} is the unit vector in the direction of observation, \mathbf{d} is the unit vector along the atomic dipole moment, \mathbf{r} is the observation point, measured from the position of the atom, and ω_0 is the polarization frequency. More details can be found, for instance in Ref. [16]. The resultant formulas are

$$S_{vis}(\omega) = \frac{C\omega_{vis}^4}{\pi} Re \int_0^\infty d\tau e^{-i\omega\tau} \langle P_{vis}^-(t) \cdot P_{vis}^+(t + \tau) \rangle \quad (45)$$

$$S_{UV}(\omega) = \frac{C\omega_{UV}^4}{\pi} Re \int_0^\infty d\tau e^{-i\omega\tau} \langle P_{UV}^-(t) \cdot P_{UV}^+(t + \tau) \rangle \quad (46)$$

Here C is an unimportant constant, same for both transitions. $P_{vis}^{(-)}$ and $P_{vis}^{(+)}$ ($P_{UV}^{(-)}$ and $P_{UV}^{(+)}$) are negative and positive frequency parts of the polarization induced on the visible(ultraviolet) transition. According to our scheme they are defined as

$$P_{vis}^-(t) = \wp_{ac}\sigma_{ac}(t) + \wp_{bc}\sigma_{bc}(t) \quad (47)$$

$$P_{vis}^+(t + \tau) = \wp_{ca}\sigma_{ca}(t + \tau) + \wp_{cb}\sigma_{cb}(t + \tau) \quad (48)$$

Similarly we define the negative- and positive-frequency parts of the polarization on the ultraviolet transition:

$$P_{UV}^-(t) = \wp_{ad}\sigma_{ad}(t) \quad (49)$$

$$P_{UV}^+(t + \tau) = \wp_{da}\sigma_{da}(t + \tau) \quad (50)$$

In the following we assume $\wp_{ac} = \wp_{ca} = \wp_{bc} = \wp_{cb}$ and $\wp_{ad} = \wp_{da}$.

Operators of atomic transitions σ_{ij} are defined in usual way: $\sigma_{ij} = |i\rangle\langle j|$. They are particularly relevant for the calculation of multi-time correlation functions. Note that these quantities are quantum-mechanical operators. Their quantum-mechanical average has simple relation to the elements of the density matrix, namely

$$\begin{aligned} \langle \sigma_{ij}(t) \rangle &= Tr[U^+(t)\sigma_{ij}(0)U(t)\rho(0)] \\ &= Tr[\sigma_{ij}(0)U(t)\rho(0)U^+(t)] \\ &= Tr[\sigma_{ij}(0)\rho(t)] \end{aligned} \quad (51)$$

Since we need to calculate two-time correlation functions, it is instructive to write down equations of motion for relevant operators and then find solutions to the initial-value problem. The form of these equations coincide with the equations of motion for respective density matrix elements.

This can be checked by direct derivation from the Heisenberg equation of motion with the Hamiltonian [8]. Thus we get

$$\sigma_{ac} = -\frac{1}{2}(3r_{vis} + r_{UV} + r_e + \gamma_{vis} + \gamma_{UV})\sigma_{ac} - \frac{1}{2}r_{vis}\sigma_{bc} \quad (52)$$

$$\sigma_{bc} = -\frac{1}{2}(3r_{vis} + r_{UV} + r_e + \gamma_{vis})\sigma_{bc} - \frac{1}{2}r_{vis}\sigma_{ac} \quad (53)$$

$$\sigma_{ad} = -\frac{1}{2}(r_{vis} + r_{UV} + r_e + \gamma_{vis} + \gamma_{UV})\sigma_{ad} \quad (54)$$

endalign where we used the assumption $r_a = r_b \equiv r_{vis}$. Note that $\sigma_{ji} = \sigma_{ij}^\dagger$ and the equations of motion for the conjugate operators arise by taking the Hermite conjugate of the right-hand sides of Eqs. (52)-(54). The above equations form the closed system and allow simple solutions. These solutions acquire even simpler form when we apply our key inequality (34). Thus, for the quantities of interest we get

$$\sigma_{ca}(t + \tau) + \sigma_{cb}(t + \tau) = e^{-\frac{1}{2}r_0\tau} [\sigma_{ca}(t) + \sigma_{cb}(t)] \quad (55)$$

$$\sigma_{da}(t + \tau) = e^{-\frac{1}{2}(r_{UV} + r_{vis})\tau} \sigma_{da}(t) \quad (56)$$

where $r_0 \equiv (2r_{vis} + r_{UV} + r_e)$.

Everything is ready for the formulation of the desired result. After substituting solution (55) in the expression (48) and correspondingly (56) in (50), the two-time correlation functions of the polarizations read

$$\begin{aligned} \langle P_{vis}^-(t) \cdot P_{vis}^+(t + \tau) \rangle &= \wp_{ac}^2 e^{-r_0\tau} \\ &\quad \times \langle \sigma_{aa}(t) + \sigma_{bb}(t) + \sigma_{ab}(t) + \sigma_{ba}(t) \rangle \end{aligned} \quad (57)$$

$$\langle P_{UV}^-(t) \cdot P_{UV}^+(t + \tau) \rangle = \wp_{ad}^2 e^{-(r_{UV} + r_{vis})\tau} \langle \sigma_{aa}(t) \rangle \quad (58)$$

The Fourier transform of the above expressions converts the exponential decays in time to the Lorentzian spectra in frequency:

$$S_{vis}(\omega) = \frac{C\omega_{vis}^2 \wp_{ac}^2}{\pi} \frac{r_0}{\omega^2 + r_0^2} 2\rho_{BB}(t) \quad (59)$$

$$S_{UV}(\omega) = \frac{C\omega_{UV}^2 \wp_{ad}^2}{\pi} \frac{r_{UV} + r_{vis}}{\omega^2 + (r_{UV} + r_{vis})^2} \rho_{aa}(t) \quad (60)$$

Here we take only the real part of the integral and use the rule (51) for calculating quantum-mechanical averages, and also the definition of the population of the bright state (29). Note also the equality $\rho_{ab} = \rho_{ba}$ valid for the zero value of the two-photon detuning, which is the case considered here.

Note here that it may seem that the thus obtained spectra can, in principle, become a function of time, copying the time dependence of populations ρ_{BB} and ρ_{aa} . This dependence is a signature of a nonstationary process. Therefore the spectrum of these solutions is to be defined not by Eq. (43) but with the more general formula which is derived and discussed for instance in Ref. [13]. However, in our case the interest is in stationary emission corresponding to steady-state solutions for ρ_{BB} and ρ_{aa} . Therefore, ρ_{BB} and ρ_{aa} become time

independent. In Fourier space they are simply two stationary Lorentzian peaks. Spectral-line intensities follow as the frequency integral over these peaks:

$$I_{vis} = \hbar^{-1} C \omega_{vis}^3 \wp_{ac}^2 2\rho_{BB} \quad (61)$$

$$I_{UV} = \hbar^{-1} C \omega_{UV}^3 \wp_{ad}^2 \rho_{aa} \quad (62)$$

The branching ratio is the ratio of two above quantities, as regulated by definition (2):

$$R = \frac{\gamma_{vis}}{\gamma_{UV}} \frac{2\rho_{BB}}{\rho_{aa}} \quad (63)$$

where we used the definition of the spontaneous decay constant

$$\gamma_{vis} = \frac{1}{4\pi\epsilon_0} \frac{4\omega_{vis}^3 \wp_{ac}^2}{3\hbar c^3} \quad (64)$$

and similar formula for the ultraviolet transition, and canceled out common prefactors.

This ratio is the main formula of our chapter. It reflects the role of coherent effects in the spontaneous emission along the visible transition. A small population in the bright state on the background of relatively strongly populated $|a\rangle$ state implies the suppression of the spontaneous decay. Such asymmetry becomes possible only when the coherence ρ_{ab} between the two upper states $|a\rangle$ and $|b\rangle$ acquires an appreciable value. Here, the coherence is induced by collisions and its large value is guaranteed by the inequality (34), which means that decay processes destroying the coherence are of little importance. Quantitatively, the degree of the suppression is related to the value of R in absence of the interference terms which becomes simply the double ratio of decay constants, as we show below.

V. SUPPRESSION OF THE SPONTANEOUS DECAY

The branching ratio given by Eq. (63) is now the subject of the analysis with respect to the experimental observations in Ref. [12]. First of all we use steady-state values of populations given by solutions (36) and (38) in Eq. (63) and obtain

$$R = \gamma_{vis} \left(\frac{4}{r_e} + \frac{1}{r_{vis}} \right) \quad (65)$$

The common factor ρ_{cc} has been canceled out. According to the experimental observations in Ref. [12], the branching ratio was measured as the function of electron density. One order of magnitude increase in the electron density resulted in one order of magnitude decrease in the branching ratio. Let us see how such dependence emerges from the above equation.

The decay constant γ_{vis} depends nontrivially on the frequency and the dipole moment, see Eq. (64). Within the range of change of the experimental conditions, no dependence of the transition frequency (i.e., no line shift) on electron density was found. Some theoretical efforts were made

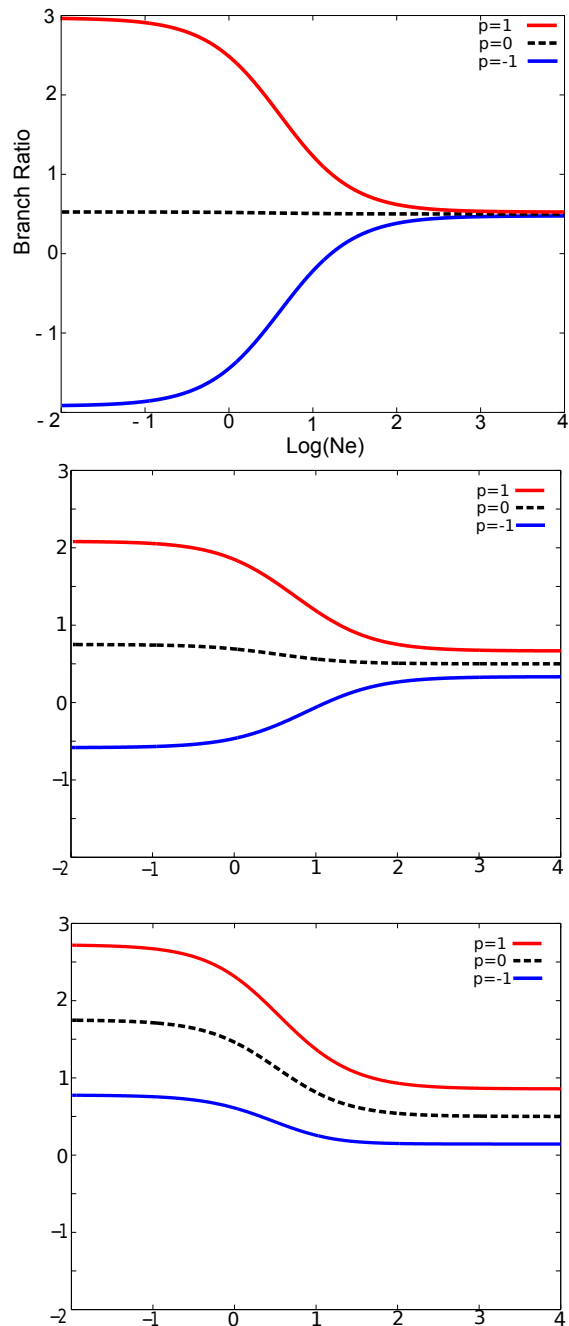


FIG. 2: The dependence of the branching ratio on logarithm of electron density. $\gamma_{uv} = 0.1\gamma_{vis}, \gamma_{uv} = \gamma_{vis}, \gamma_{uv} = 5\gamma_{vis}$.

in Ref. [17] to take into account the effect of the screening of the atomic potential by the surrounding plasma. This effect can, in principle, modify the Coulomb field experienced by the valence electron and, thus, significantly change the transition probability (i.e. dipole moment). However, this change becomes of an appreciable value only for concentrations much higher than that used in the experiment. So, we conclude that no change takes place in the value of γ_{vis} when concentration varies.

The observed changes of the branching ratio R in Ref.

[12] can be attributed mainly to the dependence of collisional rates r_e and r_{vis} (and, of course r_{UV}) on the density of free electrons. Apparently the higher the density the more frequently the collision events occur and therefore the larger the rates. More precisely, we assume linear dependence of the collisional rates on the concentration ($r_i \propto N$) and write for a constant electron temperature

$$r_i(N) = k_i N \quad (66)$$

where $i = e, vis, UV$, and k_i is the proportionality coefficient. Typical range of concentrations where the effect occurs covers the region $10^{18} - 10^{19} cm^{-3}$. Applying dependences given by Eq. (66) to Eq. (65), we perform simulation and present obtained results in Fig. 2. We thus illustrate main result of our study - the sensitive dependence of the branching ratio on the concentration. The range of the change is of the same order as was observed in the experiments.

For completeness we analyze the dependence of the collisional rates (and therefore, the branching ratio) on the electron temperature of plasma. This dependence, even when present, cannot be deduced from the experiments in Ref. [12] where the electron temperature was estimated as constant under operating conditions and equal to $\approx 5eV$. However, in the set of related experiments on measurements of the branching ratio in high-density plasmas of CIII performed in a later work in Ref. [18], the temperature varied considerably and, therefore, we can expect a well pronounced dependence of the branching ratio on the temperature. Thus for the concentration $0.7 \times 10^{18} cm^{-3}$, the temperature was 5.7 eV; while for higher concentration $2.6 \times 10^{18} cm^{-3}$, the temperature increased to 9.3eV.

It is instructive to analyze the simultaneous electron density and temperature dependences. Free electrons in plasmas obey the classical Boltzmann distribution thus the number of particles dN (in a unit volume) within the range of energies $E + dE$ yields

$$dN = N \frac{2}{\sqrt{\pi}} \frac{1}{(kT)^{3/2}} e^{-\frac{E}{kT}} \sqrt{E} dE \quad (67)$$

So, for collisional rates we can write

$$r_i(N, T) = 2N \bar{k}_i \sqrt{\frac{2kT}{\pi M}} e^{-\frac{E_i}{kT}} \quad (68)$$

where \bar{k}_i is a cross-section. Then the coefficient k_i is given by

$$k_i = 2\bar{k}_i \sqrt{\frac{2kT}{\pi M}} e^{-\frac{E_i}{kT}} \quad (69)$$

The branching ratio was measured in Ref. [18] for five concentration/temperature points.

VI. SIMULATION RESULTS

We have performed numerical simulation to demonstrate the dependency of branch ratio on electron density. For purposes of plasma diagnostics, we simulate the situation with

or without the coherent effects due to electron impacts, depending on the relative orientation of the dipole moments of optical and UV transitions.

Here we assume that $\gamma_{vis} = 1$, so that all the other parameters are normalized by γ_{vis} . The collision-induced incoherent pumping rates are dependent on electron density; here we use $r_{UV} = 0.001 \times N_e$, $r_e = 0.1 \times N_e$, and $r_v = 0.3 \times N_e$. We considered three different UV decay rates with $\gamma_{UV} = 0.1, 1, 5$ to investigate the dependence of branching ratio on electron density.

Fig.2.(a) corresponds to small UV decay rate $\gamma_{UV} = 0.1\gamma_{vis}$. Fig.2.(b,c) correspond to larger UV decay rate $\gamma_{UV} = 1, 5$ respectively. In each figure, the top red curve is for $p = 1$, the bottom blue curve is for $p = -1$, and the dashed line is for $p = 0$.

Through these nine curves, we notice that, at large electron density, the dependence of the branching ratio on density for different p factors behave in a similar way and trend to 0.5. In the special case with $p = 0$, this process gets to limit much more quickly. It is also clear that with larger UV decay rate, the dependence of the branching ratio on density for different p factors also behaves very similarly, but at a lower decay rate. At both sides of the extremely low or high electron density, there clearly limits. Outside this range, the electron density has no effect on the branching ratio.

Obvious conclusion from the comparison of curves is that the increase of temperature greatly suppresses variations in the branching ratio with concentration. The relatively small slope of the curve could be the reason or one of the reasons that yielded the very weak concentration dependence and led the experimenters in Ref. [18] to the conclusion of the absence of the dependence of the branching ratio on the concentration.

We thus complete the comparison with the experiments. On our way to the main result expressed by formula (65) we made two important assumptions. One is the condition of maximal coherence. The other is the domination of collisional rates over all relevant decays, see Eq. (34). It is instructive now to see what happens if we relax the first assumption and consider the opposite case - the case of no coherence. Simply set p factor to zero; that is equivalent to setting $\rho_{ab} = 0$ (at least in the steady-state). Given inequality (34), two upper states $|a\rangle$ and $|b\rangle$ are populated equally in steady state. In the case of no coherence, the population of the bright state is simply one half of the sum of ρ_{aa} and ρ_{bb} . So, we get

$$\rho_{aa} \approx \rho_{bb} \approx \left(1 + \frac{r_e}{2r}\right) \rho_{cc} \quad (70)$$

With these solutions in Eq. (63), we finally obtain

$$R \approx 2 \frac{\gamma_{vis}}{\gamma_{UV}} \quad (71)$$

for the branching ratio for the visible and ultraviolet transitions in the case of no coherence between two upper states $|a\rangle$ and $|b\rangle$. This value is considerably larger than the branching ratio obtained for the case of maximal coherence, see Eq. (65). Moreover, this value does not depend on collisional rates and therefore on concentration. The comparison of

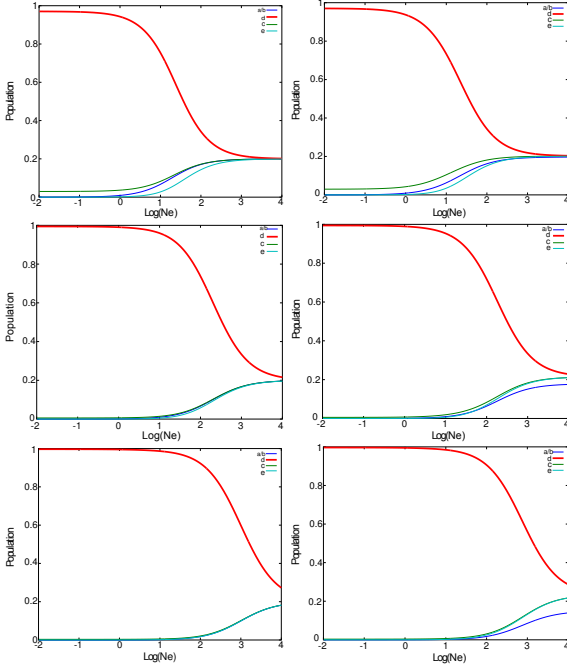


FIG. 3: The dependence of the populations on logarithm of electron density. $\gamma_{uv} = 0.1\gamma_{vis}$, $p = 0$, $\gamma_{uv} = \gamma_{vis}$, $p = 0$, $\gamma_{uv} = 5\gamma_{vis}$, $p = 0$

branching ratios calculated for these two cases demonstrates the key role of coherence in interpreting experimental results obtained in Ref. [12].

VII. ANALYTICAL SOLUTIONS

Analytical solutions can be derived from dynamical equations of population densities, ie Eq. (9-16). We obtain

$$\rho_d = \frac{r_{uv} + \gamma_{uv}}{r_{uv}} \rho_a = R_{da} \rho_a \quad (72)$$

$$\rho_e = \frac{r_e}{r_e + 2\gamma_e} \rho_c = R_{ec} \rho_c \quad (73)$$

$$\rho_a = \rho_b \quad (74)$$

$$\rho_{ab} = \frac{Pr_v}{\Gamma_{ab}} (\rho_c - \rho_a) \quad (75)$$

where

$$\Gamma_{ab} = r_v + g_v + g_{uv}/2 \quad (76)$$

and

$$\rho_c = R_{ca} \rho_a \quad (77)$$

where we introduce

$$R_{ca} = \frac{2(r_v + g_v - P^2 r_v^2 / \Gamma_{ab})}{2r_v + r_e - r_e R_{ec} - 2P^2 r_v^2 / \Gamma_{ab}} \quad (78)$$

Here we can use the conservation of the electron number. Suppose that the total number of electrons in all levels is

$$\rho_a + \rho_b + \rho_c + \rho_d + \rho_e = 1 \quad (79)$$

Thus we get

$$\rho_a = \frac{1}{2 + R_{ca} + R_{da} + R_{ec} R_{ca}} \quad (80)$$

By exploiting the relationships of density between different levels, we can find each level's density.

It is known that the density of the bright state is defined as

$$\rho_{BB} = \rho_a + \rho_b + 2\rho_{ab} \quad (81)$$

and the definition of the branch ratio is

$$R \approx \frac{\rho_{BB}}{\rho_a} \quad (82)$$

By using all the results we have obtained, we finally get the expression of the branch ratio

$$R = 2 + \frac{2Pr_v}{\Gamma_{ab}} (2R_{ca} - 1) \quad (83)$$

It can be noticed that the branching ratio Limit, at low and high electron densities is

$$R = \begin{cases} 1 + 2\frac{\gamma_v}{\gamma_{UV}} & N_e \rightarrow 0 \\ 2\frac{\gamma_v}{\gamma_{UV}} & N_e \rightarrow \infty \end{cases} \quad (84)$$

With no coherence excited by electron collisions, the ratio is given by

$$R = \frac{\gamma_v(\gamma_{UV} + 2(\gamma_v + r_v))}{\gamma_{UV}(\gamma_v + r_v)} \quad (85)$$

VIII. DISCUSSION

So far we discussed the suppression of spontaneous decay on the visible transition. This suppression is due to the two-photon coherence induced by the interference of collision processes along two overlapping optical transitions $|a\rangle - |c\rangle$ and $|b\rangle - |c\rangle$. In order to quantify the degree of the suppression we introduced the branching ratio as the ratio of total spectral-line intensities for the two transitions. Here, one transition is the visible transition (actually, simultaneously two transitions) of interest and the other transition is the reference ultraviolet transition. This branching ratio calculated for the case of maximal two-photon coherence, see Eq. (65), is compared to the branching ratio evaluated for

the case of no coherence, see Eq. (71). The degree of the coherence-induced suppression can be deduced as the ratio of these two branching ratios.

This study demonstrates the possibility of coherent effects in plasmas, where the coherence is induced by the interference of incoherent processes. Here the collisions of free electrons with ions represent these incoherent processes, and they indeed happen rather frequently for concentrations as high as 10^{18}cm^{-3} . When they dominate over relevant decay rates, the two-photon coherence becomes of substantial value that leads to efficient suppression of the spontaneous emission on the visible transition. This suppression was registered experimentally and reported by Chung, Lemaire, and Suckewer in Ref. [12]. Moreover, we are able to explain sensitive dependence of the degree of suppression on concentration of free electrons. It is interesting that the dependence on

the concentration only appears due to the collision-induced coherence and disappears in the absence of the coherence, as comparing Eqs. (65) and (71) shows.

IX. ACKNOWLEDGEMENT

We thank Marlan Scully for his support on this work. This work is supported by the Robert. A. Welch Foundation (Grant A-1261), D. S. thanks the support from the Fujian Provincial Natural Science Foundation(2018I0019), Science Technology innovation project of Xiamen(3502Z20183062), Y.R. gratefully acknowledges the support from the UNT Research Initiation Grant.

-
- [1] V. Weisskopf and E. Wigner, *Z. Phys.* 63, 54 (1930); 65, 18 (1931).
 - [2] S. Haroche and D. Kleppner, *Phys. Today* 44(1), 24 (1989).
 - [3] E. M. Purcell, *Phys. Rev.* 69, 681 (1946).
 - [4] P. Goy, J. M. Raimond, M. Gross, and S. Haroche, *Phys. Rev. Lett.* 50, 1903 (1983).
 - [5] D. Kleppner, *Phys. Rev. Lett.* 47, 233 (1981).
 - [6] D. A. Cardimona, M. G. Raymer, and C. R. Stroud, *J. Phys. B* 15, 55 (1982).
 - [7] L. M. Narducci, M. O. Scully, G.-L. Oppo, P. Ru, and J. R. Tredicce, *Phys. Rev. A* 42, 1630 (1990).
 - [8] D. J. Gauthier, Y. Zhu, and T. W. Mossberg, *Phys. Rev. Lett.* 66, 2460 (1991).
 - [9] S. Y. Zhu and M. O. Scully, *Phys. Rev. Lett.* 76, 388 (1996).
 - [10] H. Lee, P. Polynkin, M. O. Scully, and S.-Y. Zhu, *Phys. Rev. A* 55, 4454 (1997).
 - [11] S. E. Harris, *Phys. Rev. Lett.* 62, 1033 (1989).
 - [12] Y. Chung, P. Lemaire, and S. Suckewer, *Phys. Rev. Lett.* 60, 1122 (1988).
 - [13] M. O. Scully and M. S. Zubairy, *Quantum Optics*, Cambridge University Press, Cambridge, 1997.
 - [14] M. Fleischhauer, C. H. Keitel, M. O. Scully, and C. Su, *Opt. Commun.* 87, 109-114 (1992).
 - [15] V. V. Kozlov, Yu. Rostovtsev, M. O. Scully, *Phys. Rev. A* 74, 063829 (2006).
 - [16] L. M. Narducci, M. O. Scully, G.-L. Oppo, P. Ru, and J. R. Tredicce, *Phys. Rev. A* 42, 1630 (1990).
 - [17] Y. Chung, H. Hirose, and S. Suckewer, *Phys. Rev. A* 40, 7142 (1989).
 - [18] S. Glenzer, J. Musielok, and H.-J. Kunze, *Phys. Rev. A* 44, 1266 (1991).
 - [19] M. O. Scully, *Advances in Multi-photon Processes and Spectroscopy*, 14, pp 126-132 (1999)